Identification and Quantification of Nanoplastics in Surface Water and Groundwater by Pyrolysis Gas Chromatography-Mass Spectrometry

Xu, Yanghui; Ou, Qin; Jiao, Meng; Liu, Gang; Van Der Hoek, Jan Peter

DOI
10.1021/acs.est.1c07377

Publication date
2021

Document Version
Final published version

Published in
Environmental Science and Technology

Environmental Science & Technology

pubs.acs.org/est

Article

Identification and Quantification of Nanoplastics in Surface Water and Groundwater by Pyrolysis Gas Chromatography−Mass Spectrometry

Yanghui Xu, Qin Ou, Meng Jiao, Gang Liu,* and Jan Peter van der Hoek

Cite This: *Environ. Sci. Technol.* 2022, 56, 4988−4997

Read Online

ACCESS | Metrics & More | Article Recommendations | Supporting Information

ABSTRACT: Nanoplastics (NPs) are currently considered an environmental pollutant of concern, but the actual extent of NP pollution in environmental water bodies remains unclear and there is not enough quantitative data to conduct proper risk assessments. In this study, a pretreatment method combining ultrafiltration (UF, 100 kDa) with hydrogen peroxide digestion and subsequent detection with pyrolysis gas chromatography−mass spectrometry (Py-GC/MS) was developed and used to identify and quantify six selected NPs in surface water (SW) and groundwater (GW), including poly(vinylchloride) (PVC), poly(methyl methacrylate) (PMMA), polypropylene (PP), polystyrene (PS), polyethylene (PE), and poly(ethylene terephthalate) (PET). The results show that the proposed method could detect NPs in environmental water samples. Nearly all selected NPs could be detected in the surface water at all locations, while PVC, PMMA, PS, and PET NPs were frequently below the detection limit in the groundwater. PP (32.9−69.9%) and PE (21.3−44.3%) NPs were the dominant components in both surface water and groundwater, although there were significant differences in the pollution levels attributed to the filtration efficiency of riverbank, with total mass concentrations of 0.283−0.793 μg/L (SW) and 0.021−0.203 μg/L (GW). Overall, this study quantified the NPs in complex aquatic environments for the first time, filling in gaps in our knowledge about NP pollution levels and providing a useful methodology and important reference data for future research.

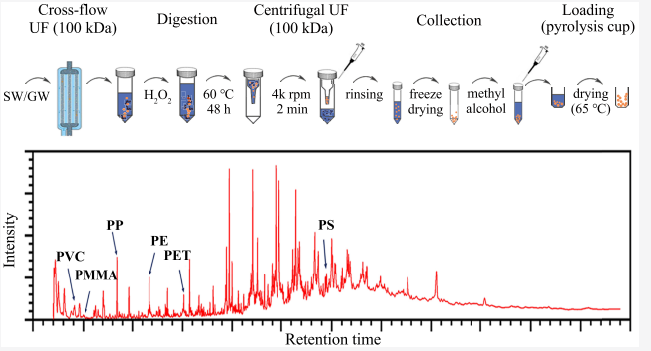

KEYWORDS: *nanoplastics, quantification, surface water, groundwater, Py-GC/MS*

INTRODUCTION

As emerging pollutants, microplastics (MPs) and nanoplastics (NPs) have attracted extensive attention and discussion.[1−9] Defined by their sizes, MPs refer to plastics between 1 μm and 5 mm, while NPs refer to plastics smaller than 1 μm, both of which may come from many consumer products and can be additionally released as secondary products from plastic wastes due to photochemical, mechanical, and/or biological degradation processes.[1,10−14] Generally, NPs are distinguished from MPs due to differences in size, transport characteristics, interactions with environmental media, bioavailability, and ecological risks.[15] NPs are expected to exhibit more colloidal properties than MPs, and the dominant effect of Brownian motion rather than density makes them undergo distinct transport processes in aquatic systems.[15,16] NPs were reported to exhibit higher toxicity to aquatic organisms than MPs because biouptake, accumulation, and transfer across cell membranes can be easily realized when the particle size reaches nanometers.[17−21] Recent studies have investigated the environmental behavior and fate of NPs in aquatic environments[1,22−29] as well as their toxicities to aquatic organisms.[8,17,30−33] However, almost all experiments were carried out at designed concentrations of artificial NPs. Although the concentrations and distributions of MPs have been well studied, there are hardly any data on NPs in water bodies, which can be attributed to the challenges in the identification and quantification of NPs.

To date, a variety of analytical techniques have been used to determine MPs in environmental samples, but these methods are no longer applicable once the particle size reaches the nanoscale. Fourier transform infrared (FTIR) and Raman spectroscopies are the two most commonly used techniques for identifying plastic particles and estimating the size and shape of individual particles.[34−37] However, the size detection limits for FTIR microscopy and Raman microspectroscopy are ~20 and 1 μm, respectively, which limit their application in the

Received: October 29, 2021
Revised: March 24, 2022
Accepted: March 25, 2022
Published: April 4, 2022

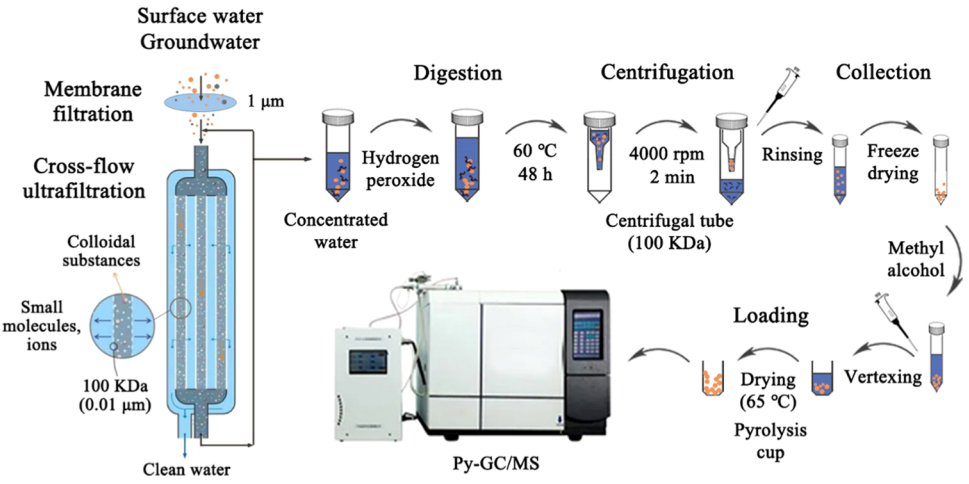

Figure 1. Pretreatment processes of water samples for NP detection by Py-GC/MS.

detection of NPs.[35,38,39] A recent study reported that combining Raman microspectroscopy with field-flow fractionation (FFF) shows potential for analyzing NPs with particle sizes down to 200 nm.[40] However, in addition to its limitations in determining NPs at smaller sizes (<200 nm), it remains unclear whether this technique could detect NPs in real-world samples. Thermal analytical methods, such as pyrolysis gas chromatography−mass spectrometry (Py-GC/MS), that quantify MPs and NPs by mass concentration are not limited by particle sizes but often require larger particle masses than spectroscopic methods.[41,42] Py-GC/MS, which is commonly used to determine the compositions and concentrations of MPs in environmental samples,[41,43−45] can be a promising technique for identifying and quantifying NPs if combined with proper pretreatment methods, such as hydrogen peroxide digestion, to minimize the possible interference of organic impurities.

Several studies have attempted to use Py-GC/MS to determine NPs in environmental and biological samples. Ter Halle et al. concentrated the colloidal fraction of 1 L seawater with a 10 kDa ultrafiltration device and identified several polymer components. However, this did not include quantification.[46] Ultrafiltration with a molecular weight cutoff of 10 kDa can remove some natural organic matter (NOM), while residual NOM may interfere with the identification and quantification of NPs.[46] Another study reported that polypropylene (PP) NPs can be directly identified, while polystyrene (PS) NPs can be determined after removing the NOM by H_2O_2/UV, but no further quantification of PP and PS NPs was conducted.[47] Zhou et al. proposed a cloud-point extraction (CPE) method for the preconcentration of trace NPs in environmental water samples.[48] The authors found that the recovery rate of standard PS and poly(methyl methacrylate) (PMMA) NPs was high, but their concentrations were far below the method's detection limits. Recently, alkaline digestion and protein precipitation were proposed for extracting NPs from aquatic animal tissues, which were then successfully quantified by Py-GC/MS.[49]

The above-mentioned efforts have made significant progress in NP research, yet the levels of NPs in environmental water bodies are still unknown due to the low concentration of NPs and the interference of NOM. As a result, proper pretreatment to concentrate NPs and eliminate interference prior to being combined with Py-GC/MS is greatly needed. Crossflow ultrafiltration could be a feasible pretreatment step because of its capacity for removing small molecular NOM and high efficiency for concentrating large volumes of water.[50] To further reduce the potential interference of other organic substances, an additional digestion method, such as H_2O_2 digestion, which is a mild and effective pretreatment method used for the extraction of MPs from organic-rich environmental matrices is necessary.[51−53]

The present study aimed to identify and quantify NPs in aquatic environments by the Py-GC/MS technique after pretreatment by ultrafiltration (100 kDa, approximately 10 nm) followed by H_2O_2 digestion. First, six selected plastic standards were investigated to determine their characteristic indicator products and respective ions to facilitate the identification and quantification. Then, the preconcentration of a large volume of water by crossflow ultrafiltration and further digestion were conducted to extract trace NPs in complex field water samples. Finally, the mass concentrations of the six selected types of NPs were successfully determined for surface water samples from six locations along a river and from the connected groundwater.

MATERIALS AND METHODS

Materials. A total of six different plastics poly(vinylchloride) (PVC), PMMA, polypropylene (PP), PS, polyethylene (PE), and poly(ethylene terephthalate) (PET) were selected, as these polymers are widely found in aquatic environments. A dispersion of PS nanoparticles (nominal size 200 nm) was purchased from Beijing Zhongkeleiming Technology Co. Ltd. PVC (CAS 9002-86-2), PMMA (CAS 9011-14-7), PP (CAS 9003-07-0), PS (CAS 9003-53-6), PE (CAS 9002-88-4), and PET (CAS 25038-59-9) were purchased from Macklin Biochemical Co., Ltd (Shanghai, China). The polymer granules or powders were frozen with liquid nitrogen, milled with a grinder for 30 min, and separated with a 500 mesh stainless steel sieve to harvest fine polymer powders. Direct weighting of small quantities of polymer powders when preparing the low calibration concentrations was difficult. To address this, the polymer powders were dispersed in a mixture of dichloromethane and methyl alcohol to facilitate the weighing of small quantities of polymers. As described in Text S1, the stock solutions (10 g/L) were continuously diluted to obtain 2−1000 mg/L plastic dispersions.

https://doi.org/10.1021/acs.est.1c07377
Environ. Sci. Technol. 2022, 56, 4988−4997

Sampling. The Fuhe River is the second largest river in Jiangxi Province (Jiangxi, China). It has a total length of 349 km and a total watershed area of 171.86 million square kilometers. In this study, six locations from upstream to downstream of the Fuhe River were chosen as sampling sites. At each sampling site, surface water and riverside groundwater were collected. A hydrogeological survey of the study area confirmed that there is a connection between the groundwater and the river water. Details about the location, distance, water level, and water quality parameters of the sampling sites can be found in the Supporting Information (Figure S1 and Table S1). Prior to sampling, the airtight PE plastic buckets (25 L) were washed several times with ultrapure water to avoid possible plastic contamination. At each sampling site, 200 L of surface water was extracted with a pump 2 m from the shore and 0−30 cm deep and collected in plastic buckets. Riverside groundwater (200 L) was drawn from local pumping wells with a stainless steel submersible pump and fed into plastic buckets. All samples were delivered to the laboratory within 1 day.

Sample Pretreatment. As shown in Figure 1, double ultrafiltration with crossflow ultrafiltration and centrifugal ultrafiltration tubes followed by hydrogen peroxide digestion was used to extract NPs. Each of the collected water samples was first passed through a 1 μm membrane filter and then concentrated by a crossflow ultrafiltration system. The detailed steps can be found in the Supporting Information (Text S2). The possible agglomerated NPs filtered out by the first step of membrane filtration (>1 μm) were generally considered MPs and excluded from the downstream analysis. Each of the concentrated water samples contains NPs and other organic matter, which may interfere with the determination of NPs by Py-GC/MS. To further minimize the possible interference from organic substances, hydrogen peroxide digestion followed by tube-type centrifugal ultrafiltration (molecular weight cutoff of 100 kDa) was used to remove organic impurities. Briefly, 5 mL of hydrogen peroxide was added to a 50 mL concentrated water sample and held for 48 h in a 60 °C water bath. After cooling, the water sample was put into a centrifugal ultrafiltration tube and centrifuged at 4000 rpm for 2 min, and the retentate was placed in a 10 mL centrifuge tube. To minimize sample loss, 2 mL of ultrapure water was injected into the centrifugal ultrafiltration tube, and then the membrane surface was gently blown with air through a pipette tip. This step was repeated three times, and the washing liquid was mixed with the previous retentate. The treated sample was freeze-dried to obtain a powder containing the NPs. This sample was added to 2 mL of methanol and vortex-mixed for 20 s to resuspend. The final suspension was repeatedly transferred into a pyrolysis target cup of 80 μL and dried in an oven at 60 °C to ensure that all of the NPs were loaded for subsequent Py-GC/MS measurement.

Dynamic Light Scattering (DLS) Measurement. The particle size distributions of NPs in surface water and groundwater samples were characterized by DLS using a Malvern Zetasizer instrument (Nano ZS, Malvern, U.K.) with a He−Ne laser at a wavelength of 633 nm and a fixed scattering angle of 90°.[29] All water samples after cross-flow ultrafiltration and after centrifugal ultrafiltration were analyzed. Prior to measurement, the concentrated water samples were sonicated in a water bath for 15 min to minimize errors caused by sample concentration. The suspension (3 mL) was added to the polystyrene DLS cuvette. The measurements were conducted in triplicate for each water sample owing to the high heterogeneity of the environmental samples.

Pyrolysis Gas Chromatography−Mass Spectrometry. Measurements were performed with a Multi-Shot Pyrolyzer EGA/PY-3030D (Frontier Laboratories, Saikon, Japan) attached to an Agilent 7890A Gas Chromatograph (Santa Clara, CA) equipped with an HP-5MS column linked to an Agilent 5975C mass spectrometer detector. The operating parameters chosen for the Py-GC/MS analysis were based on the parameters used in previous studies.[44,49] Briefly, the samples were pyrolyzed in the single-shot mode at 650 °C for 0.2 min. Pyrolysis products were injected with a split ratio of 50:1, and the pyrolyzer interface temperature was set at 320 °C. Additional details on the single-shot Py-GC/MS conditions are presented in the Supporting Information (Table S2).

The six selected polymers were analyzed by Py-GC/MS to determine their characteristic components and ions (Table S3). For PVC, only benzene (m/z 78) had a high peak intensity and sensitivity while the sensitivity of other components was not enough, so benzene was selected as the indicator for PVC.[43,44] Methyl methacrylate (m/z 100) was considered as the indicator compound for PMMA, as it is a specific and high-sensitivity pyrolysis component.[43,44,49] 2,4-Dimethyl-1-heptene (m/z 126) was selected as the indicator ion for PP, and the molecular ion m/z 43 was chosen as the quantification ion due to its high response value. PS has three favored indicator compounds: styrene, its dimer (3-butene-1,3-diyldibenzene, m/z 208) and its trimer (5-hexene1,3,5-triyltribenzene, m/z 312). With the highest abundance, styrene is the ideal indicator for PS quantification in nonmatrix samples.[54] Since the pyrolysis of environmental constituents such as chitin and albumin can also generate styrene monomers,[49] it is unsuitable for use as the indicator component for PS. The less intensive styrene trimer is a specific indicator compound for PS, and the highly responsive molecular ion m/z 91 was selected as the quantification ion.[43] 1-Decene was chosen as the indicator ion for PE, as it was the most representative pyrolysis product having a high abundance, although several natural materials could interfere with its analysis.[44,55] For PET, benzoic acid (m/z 105) was selected as an indicator component due to its high peak intensity and sensitivity.[43,55,56]

External calibration curves were obtained by analyzing different amounts of the standard plastics (0.1−10 μg for PVC, PMMA, and PS, and 0.1−50 μg for PP, PE, and PET). The identification of the characteristic peaks of each sample was achieved by comparison of their full-scan mass spectra with the analytical pyrolysis library. The instrument limits of detection and quantification (limit of detection (LOD) and limit of quantification (LOQ)) were defined as 3 and 10 times the baseline noise (S/N = 3 and S/N = 10). The LOD and LOQ values were then converted into procedural limits based on the volume of the original tested water samples (Table S4). When a value was lower than the LOQ, half of the LOD value was used.

Possible Matrix Interference. The quantification of the NPs by Py-GC/MS was based on indirect determination by analyzing their pyrolysis products. However, these products can also be produced from natural matters present in water samples. The selectivity of the indicator compounds was tested by analyzing several selected organic materials including wood, leaf, fish, humic acid, biochar, and bacteria (Table S5).[43,55]

https://doi.org/10.1021/acs.est.1c07377
Environ. Sci. Technol. 2022, 56, 4988−4997

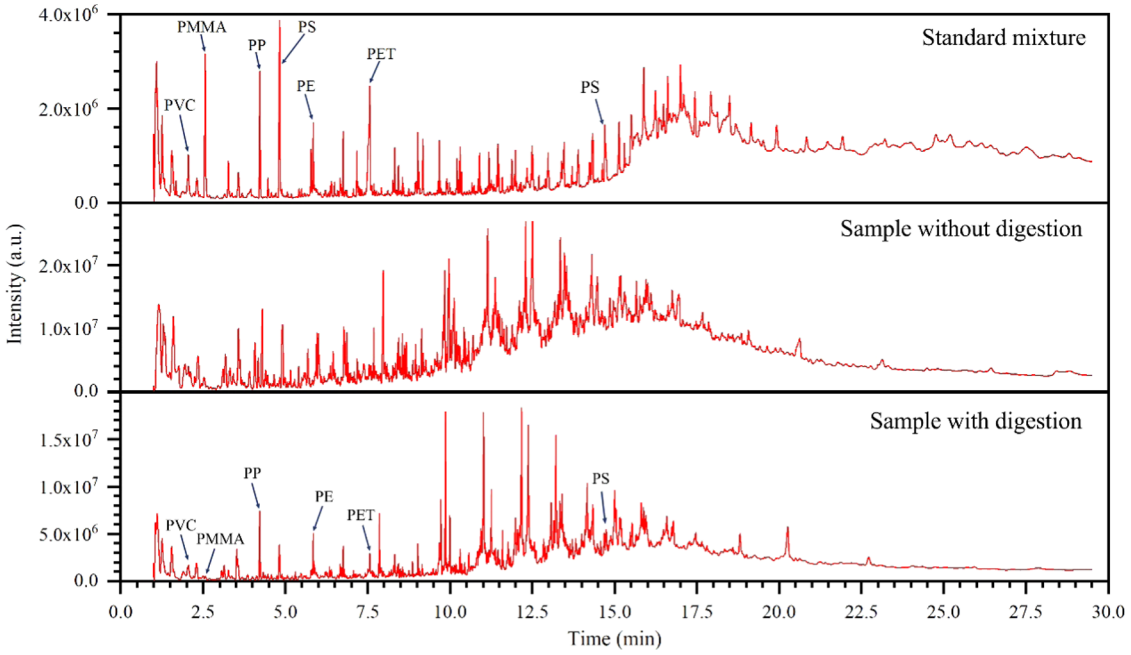

Figure 2. Chromatograms from a standard mixture and representative water samples without digestion and with digestion.

The indicator compounds for PMMA, PP and PS, and PET were not affected by these natural materials.[43,55] Wood, fish, biochar, and bacteria interfered with the analysis of PE, although these interferences were significantly decreased following the digestion procedure (Table S5). Learned from Okoffo et al.'s studies,[44,55] the occurrence of PE in samples was further confirmed based on three validation criteria: (1) the presence of a homologous series of the characteristic PE triplets (alkadiene, *n*-alkene, and *n*-alkane); (2) the presence of a homologous series of more than five triplets within C_7-C_{41} of the PE standard; and (3) the standard deviation of the peak areas of the individual C_{10} triplets is within 2 times the standard deviation of the PE standard. For the analysis of PVC, leaf and biochar caused background interference (Table S5). It was difficult to completely remove the interference for PVC because benzene is abundant in most natural matter.[43,44,55] Thus, the quantification of PVC in the water samples was potentially subject to minor bias from natural materials.

Quality Assurance/Quality Control. During sample collection, pretreatment, and measurement, special care was taken in this study to minimize possible contamination from the surrounding environment.[57] The concentration, digestion, and ultrafiltration of water samples were conducted in an ordinary laboratory, while the procedures including sample uploading and drying were carried out in a fume hood. Some plastic materials were inevitably used in sampling and sample handling, and detailed information about the compositions of these plastic materials can be found in Table S6. The plastic buckets used for sampling were carefully washed prior to sample collection. To avoid contamination that could come from the plastic items used in the experiments, polymer-free nitrile gloves (carefully washed before use) and 100% cotton lab coats were used during all steps of the analytical procedure.[35,36,58] To avoid plastic contamination from the ultrafiltration membrane, the cross-flow ultrafiltration device was run for 10 min with ultrapure water and the centrifugal ultrafiltration tubes were cleaned carefully with ultrapure water. In addition, all sample containers, such as beakers, centrifuge tubes, and pipette tips, were rinsed thoroughly three times with ultrapure water prior to use. Samples were covered with aluminum foil to avoid potential airborne contamination. All of the pyrolysis cups used for Py-GC/MS were cycled on the instrument before the addition of any sample to avoid potential contamination. Conducted with ultrapure water, three blank samples that had the same steps as the sample processing including membrane filtration, cross-flow ultrafiltration, digestion, centrifugal ultrafiltration, freeze drying, and loading were prepared and measured with Py-GC/MS. The indicator ions related to the selected polymers were not detected in blank samples or were below the limit of detection (Figure S3), suggesting that these pretreatment processes did not cause plastic contamination after careful cleaning.

RESULTS AND DISCUSSION

Py-GC/MS Analysis of Plastic Standards. The characteristic chromatograms and the mass spectra of the selected indicator compounds used for the determination of the six different plastic standards (PVC, PMMA, PP, PS, PE, and PET) are shown in Figure S4. The calibration curves of the six plastic standard polymers were positive and linear in the range of 0.1−10 μg for PVC, PMMA, and PS, and 0.1−50 μg for PP, PE, and PET with acceptable determination coefficient values ($R^2 \geq 0.98$) (Table S3). The relative standard deviations (RSDs) of the quantitative ion peak areas with five replicates for each standard sample were used to evaluate the precision of Py-GC/MS measurements. The RSDs of the six plastic polymers were determined to be 5.8−18.4% for PVC, 6.9−15.2% for PMMA, 11.3−19.0% for PP, 9.2−13.2% for PS, 6.5−16.1% for PE, and 10.1−19.6% for PET. Since most types of NPs are not yet commercially available, it is difficult to assess the recoveries of every type of NP. Commercial PS nanospheres with a particle size of 200 nm were used to represent all types of NPs for evaluating their recoveries.[59] It was found that the recovery of spiked PS NPs was 61.4 ± 13.5% (Text S3 and Table S7), indicating that the method is acceptable for detecting trace NPs in aquatic environments,

https://doi.org/10.1021/acs.est.1c07377
Environ. Sci. Technol. 2022, 56, 4988−4997

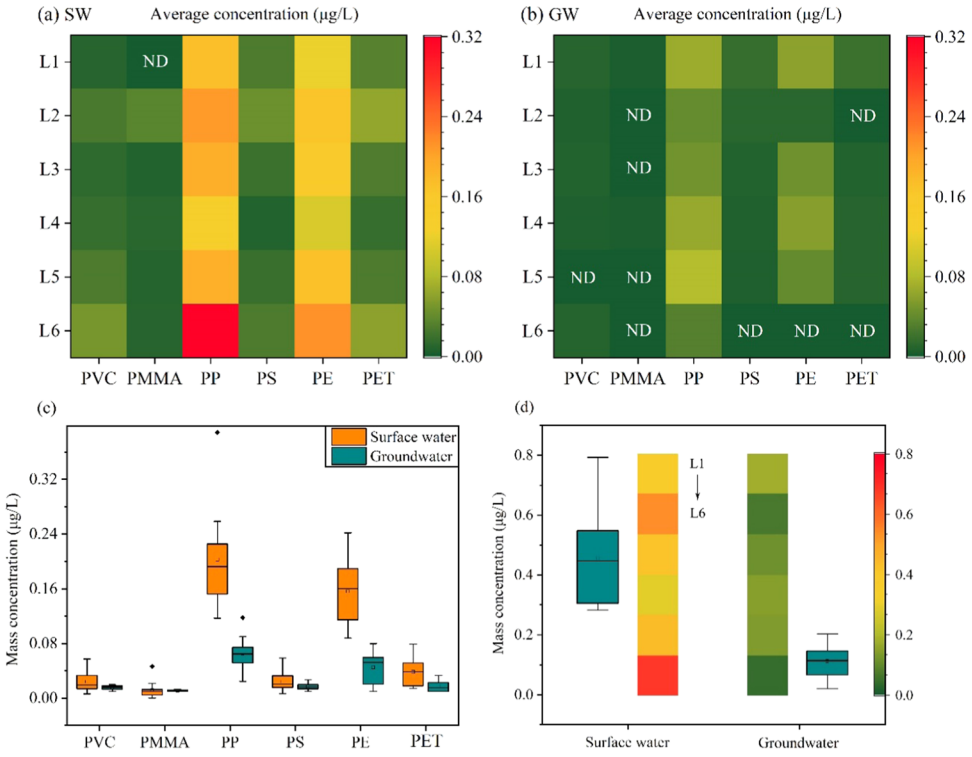

Figure 3. Heatmaps of NP average concentrations of six locations in the surface waters (a) and groundwaters (b). The boxplot of the mass concentration distributions of the selected NPs in the surface waters and groundwaters (c). Heatmap of the average concentrations of total NPs of six locations in the surface waters and groundwaters and the concentration distributions of the total NPs in the surface waters and groundwaters (d). L1, L2, ..., L6 indicate locations 1, 2, ..., 6, respectively.

especially when there are no other mature quantitative methods,[48,50] although the concentration efficiency of cross-flow ultrafiltration might not be very high.[50]

Particle Size Distributions of NPs in Environmental Water Samples. As detected by DLS, the NPs were not evenly distributed in the surface water and groundwater samples after preconcentration by cross-flow ultrafiltration (Figure S5). It was observed that several samples contained particles larger than 1 μm (Figure S5a,b), which may be due to particle agglomeration. After pretreatment with hydrogen peroxide and centrifugal ultrafiltration (100 kDa), the particle size distributions of all samples were relatively uniform and homogeneous, and there were no particles larger than 1 μm (Figure S5c,d). In addition, the peaks were mostly between 200 and 800 nm, indicating that the NPs in both surface water and groundwater were dominated by particles in this size range. Previously, it was reported that DLS could not detect colloidal substances in raw water samples due to their low concentrations in environmental samples.[46] Ter Halle et al. tried to characterize the particle size distribution of NPs in concentrated seawater samples but failed to obtain accurate size distributions, although several highly dispersed populations of nanoparticles appeared.[46] The results of the present study reveal that pretreatment by H_2O_2 combined with UF preconcentration is a critical step for the successful characterization of the particle size distributions of NPs. It should be mentioned that the membrane filtration step prior to ultrafiltration and hydrogen peroxide digestion may filter out the portion of agglomerated NPs larger than 1 μm (falls into the category of MPs). The exclusion of those NPs may slightly underestimate the amount of NPs in water samples either by mass concentration or number concentration.

Mass Concentration of NPs in Surface Water and Groundwater. The direct identification and quantification of NPs were achieved by combining H_2O_2 digestion of large volume crossflow UF concentrated retentate, followed by Py-GC/MS analysis based on pyrolysis products, characteristic ions, and their corresponding intensities. The chromatograms of the standard mixture and water samples without and with digestion are shown in Figure 2. Figure 2a shows that the six selected plastic polymers can be clearly distinguished in a mixed standard sample according to the components' presence at different retention times. For the cross-flow UF concentrated samples, although some components could be identified, the chromatogram was complicated, which could be attributed to the presence of residual NOM interfering with NP identification. After H_2O_2 digestion and further ultrafiltration, the chromatogram contained fewer noise peaks, and similar pyrolysis products at the same retention times were observed (Figure 2).

Based on the similarity analysis of these peaks, all selected NPs (PVC, PMMA, PP, PS, PE, and PET) were successfully identified in surface water and groundwater samples from the six sampling locations (Figure S6). The mass concentrations of NPs in all surface waters and groundwaters were quantified according to the corresponding peak areas (Figure 3). The results illustrate the fact that the levels of all NPs in the surface water at all six locations were significantly different from those in the groundwater (Figure 3a,b). All NPs except PMMA were detected in the surface waters of all locations, among which the concentrations of PE and PP were relatively high (Figure 3a). Figure 3c shows the concentrations of the various NPs in the surface waters and groundwaters across all locations in a boxplot. In the surface water, the NPs were dominated by PP

https://doi.org/10.1021/acs.est.1c07377
Environ. Sci. Technol. 2022, 56, 4988−4997

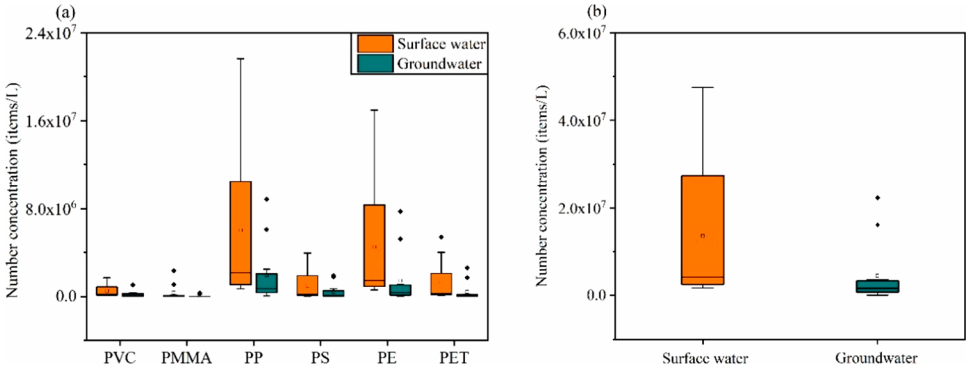

Figure 4. Number concentrations of the different NPs in the surface waters and groundwaters (a) and the total number concentrations of all of the NPs in the surface waters and groundwaters (b).

and PE, which accounted for 37.3−50.3 and 27.2−0.8% with concentrations ranging from 0.117 to 0.389 μg/L and 0.088−0.242 μg/L, respectively, followed by PET (4.5−15.6%, 0.011−0.079 μg/L), PS (2.2−12.1%, 0.007−0.058 μg/L), PVC (2.1−7.4%, 0.006−0.057 μg/L), and PMMA (0−8.1%, 0−0.046 μg/L) (Figure 3c). In general, the NP concentrations in the groundwaters were lower than those in the surface waters, and several NPs were below the detection limit in the groundwater of certain locations (Figure 3b; 4/6 PMMA, 2/6 PET, 1/6 PVC, 1/6 PE, and 1/6 PS). Similarly, PP (0.014−0.108 μg/L) and PE (0−0.070 μg/L) remained the dominant NPs in the groundwaters, accounting for 34.3−82.9 and 0−44.0%, respectively. The concentrations of PVC (0−0.010 μg/L, 0−17.1%), PMMA (0−0.003 μg/L, 0−2.1%), PS (0−0.017 μg/L, 0−19.3%), and PET (0−0.024 μg/L, 0−11.6%) were low and showed no significant differences (Figure 3c).

To the best of our knowledge, there are no available data on the levels of NPs in freshwater, although several studies have attempted to detect them.[46−48] Although not truly comparable, a previous study of snow pit and surface snow samples using thermal desorption−proton transfer reaction−mass spectrometry (TD-PTR-MS) identified and (semi)quantified plastic polymers at the nanoscale.[60] In the study, only PET was detected at 5.4−27.4 μg/L, which was much higher than PET and even the total mass of selected NPs found in the water samples of the present study. The low mass concentration of NPs in the present study might be related to the differences in the NP sources of the different environmental samples. Similar to MPs, NPs may enter surface water by pathways such as industrial and wastewater effluents, surface run-off, and atmospheric deposition.[61] Studies have suggested that freshwater MPs mainly consist of PP, PE, PET, PS, and PVC.[62,63] Among these major MPs, PP and PE with large global plastic demand and low density were dominant,[64] which agrees with the results of the NPs found in both surface water and groundwater in the present study.

Figure 3d shows the average concentrations and the concentration distributions of the total NPs in the surface waters and groundwaters at the six locations from upstream to downstream along the Fuhe River. Generally, at the same locations, the levels of NPs in the groundwaters were significantly lower than those in the surface waters (0.021−0.203 vs 0.283−0.793 μg/L, $p < 0.001$). This can be attributed to the robust filtration efficiency of the riverbank between the Fuhe River and the abstraction wells at each location.[65,66] For the surface waters, the average concentration of NPs at L1, which is the most upstream sampling site located in a rural area, was relatively low (0.364 μg/L), while at L2 and L6, the average mass concentrations of the sums of the tested NPs were higher than that at L1 (0.540 and 0.683 μg/L), which might be related to the high pollution input from these two urban regions. This hypothesis agrees with previous findings regarding MPs, which reveal that the abundance of MPs was positively correlated with economic development.[34,67] Moreover, biofouling and interaction with other environmental substances, such as metals and inorganic colloids, may facilitate the settling of NPs, while hydraulic disturbance would resuspend and release the settled NPs to the surface of the water column.[24,34,67−70] However, the cases were different for the groundwaters: the mass concentrations of the sums of the tested NPs at L1 (0.175 μg/L) were the highest, while those of L2 (0.067 μg/L) and L6 (0.040 μg/L) were the lowest (Figure 3d). The reason for such differences might be the different hydrogeological conditions and water abstraction habits within each riverbank village, which could contribute to the variable penetration and removal behavior of NPs through the riverbank.[65,71]

Understanding the Number Concentrations of the NPs. In addition to the mass concentrations, the number concentrations (number of particles per liter, items/L) is also critical to evaluate the pollution level of NPs in aquatic environments. However, it is impossible to identify and count NPs in complex environmental samples by microscopy techniques. An estimation of the number concentrations of the NPs was performed based on particle sizes, polymer densities, and the mass concentrations determined by Py-GC/MS. However, it was impossible to determine the shapes and sizes of the different NPs in the different samples. To simplify this and facilitate visualization of the number concentrations, it was assumed that all NPs were spherical. The particle sizes of each sample were determined based on the respective peak size of the DLS result for each sample. According to previous studies, the polymer densities of PVC, PMMA, PP, PS, PE, and PET were estimated to be 1.39, 1.18, 0.91, 1.05, 0.95, 1.40, and 1.15 g/cm^3, respectively.[64,72] Calculated by eq S1 (Text S4), the number concentrations (items/L) of the different NPs in surface waters and groundwaters are shown in Figure 4.

It was estimated that there were (0.2−4.7) × 10^7 NP items/L in the surface waters, which were composed of (0.99−1.7) × 10^6 PVC NP items/L, (0−2.3) × 10^6 PMMA NP items/L, (0.07−2.2) × 10^7 PP NP items/L, (0.04−4.0) × 10^6 PS NP items/L, (0.06−1.7) × 10^7 PE NP items/L, and (0.09−5.4) × 10^6 PET NP items/L (Figure 4a,b). For the groundwaters, the number concentrations were approximately an order of

https://doi.org/10.1021/acs.est.1c07377
Environ. Sci. Technol. 2022, 56, 4988−4997

magnitude lower than those of the surface waters. There were $(0.01-2.2) \times 10^7$ NP items/L, which were composed of $(0-1.0) \times 10^6$ PVC NP items/L, $(0-3.3) \times 10^5$ PMMA NP items/L, $(0.06-8.9) \times 10^6$ PP NP items/L, $(0-1.9) \times 10^6$ PS NP items/L, $(0-7.7) \times 10^6$ PE NP items/L, and $(0-2.6) \times 10^6$ PET NP items/L (Figure 4a,b). Admittedly, these figures can give us only a rough understanding of the number concentration of NPs but fail to fully represent reality because the shapes and sizes of NPs can be variable. As observed, although the mass concentrations of the NPs were rather low, the number concentrations may be much higher than those of the MPs.[62,63,73−75] Several studies also suggested that the proportion of MPs increases with decreasing particle size.[58,76] Pivokonsky et al. found that MPs of 1−5 and 5−10 μm were estimated to be $(0.8-1.7) \times 10^3$ and $(0.5-1.2) \times 10^3$ items/L in surface water, which accounted for approximately 40−60 and 30−40% of the total MP counts, respectively.[76] Thus, there can be thousands of MPs, while millions of NPs per liter in aquatic environments.

Environmental Implications. Recently, the fate, transformation, and ecological risks of NPs in aquatic environments have been extensively investigated, but information about the pollution level and distribution of NPs remains unknown due to the lack of feasible qualitative and quantitative methodologies. Several studies have attempted to quantify NPs in environmental samples using various methods,[40,46,48,49,60,77] but few were able to truly quantify the concentrations of NPs in actual samples, especially in water bodies. This study developed a feasible method to determine trace NPs in complex waters, and the contamination levels of NPs in field surface waters and groundwaters were further investigated. The six selected NPs (PVC, PMMA, PP, PS, PE, and PET) were successfully identified and quantified, of which PP and PE were dominant in all samples. The mass concentrations of the NPs in the surface waters and groundwaters were 0.283−0.793 and 0.021−0.203 μg/L, while the number concentrations were estimated to be $(0.2-4.7) \times 10^7$ and $(0.01-2.2) \times 10^7$ items/L, respectively. This study assessed the actual pollution levels of the NPs in the water bodies, which provide important reference data for other studies. For any assessment of the relevant issues, it is critical that the selected number and type of NPs reflect the actual situation. For example, most studies investigated the transport and fate of NPs in aquatic media at concentrations (e.g., 10 mg/L) much higher than the concentration of NPs detected here.[22,23,25,78−80] Moreover, commercial PS is commonly used to represent NPs for studying their environmental behaviors and biological effects,[19−21,81] but this study found that PP and PE were the dominant NPs, while PS only accounted for a small proportion.

It needs to be mentioned that the current study leaves some room for improvement although it has successfully identified and quantified trace NPs in the surface waters and groundwaters. For instance, pretreatment by H_2O_2 combined with UF preconcentration can inevitably cause some sample loss, which can underestimate the real concentration of NPs. Given its high concentration ratio, it is acceptable to quantify trace NPs in water bodies, especially when there are no other mature quantitative methods. Thus further improvements are required to better optimize extraction and treatment efficiency. Moreover, the NP recovery rates of the proposed method were only evaluated by commercial PS NPs but may vary for different NP types. Additionally, this study proposed a feasible method to detect trace NPs in water bodies, and future efforts need to be made to bridge the knowledge gap in NP contamination levels in other complex systems, such as sediment and soil environments.

■ ASSOCIATED CONTENT

Supporting Information

The Supporting Information is available free of charge at https://pubs.acs.org/doi/10.1021/acs.est.1c07377.

Determination of standard curves of selected plastics (Text S1); cross-flow ultrafiltration (Text S2); extraction and recovery efficiency of NPs (Text S3); estimation of number concentrations of the NPs in the water samples (Text S4); locations of the six sampling sites in the Fuhe River (Figure S1); water quality parameters of the sampling sites (Table S1); schematic diagram of concentrating the water samples with crossflow ultrafiltration (Figure S2); conditions for single shot Py-GC/MS measurements (Table S2); characteristic components and calibration functions of the six plastics (Table S3); LOD and LOQ of the different NPs in the water samples (Table S4); potential interferences of selected natural polymers with polymer indicator ions (Table S5); composition of the plastic materials used in sampling and sample preparation (Table S6); recovery of NPs tested with PS NPs (Table S7); densities of the different types of plastics used for number concentration estimation (Table S8); mass concentrations of PVC, PMMA, PP, PS, PE, and PET measured in the surface waters and groundwaters (Table S9); representative mass spectrum of the blank sample (Figure S3); total ion chromatogram pyrograms and mass spectra of the characteristic pyrolysis products of the six selected plastics (Figure S4); particle size distributions of the NPs in the water samples (Figure S5); Py-GC/MS chromatograms of a representative surface water and a groundwater (Figure S6); and results of similarity analysis of the characteristic peaks of a representative sample (Figure S7) (PDF)

■ AUTHOR INFORMATION

Corresponding Author

Gang Liu − *Key Laboratory of Drinking Water Science and Technology, Research Centre for Eco-Environmental Sciences, Chinese Academy of Sciences, 100085 Beijing, P. R. China; University of Chinese Academy of Sciences, 100049 Beijing, P. R. China;* orcid.org/0000-0002-4008-9017; Phone: 008617600879707; Email: gliu@rcees.ac.cn

Authors

Yanghui Xu − *Key Laboratory of Drinking Water Science and Technology, Research Centre for Eco-Environmental Sciences, Chinese Academy of Sciences, 100085 Beijing, P. R. China; Section of Sanitary Engineering, Department of Water Management, Faculty of Civil Engineering and Geosciences, Delft University of Technology, 2628 CN Delft, The Netherlands*

Qin Ou − *Key Laboratory of Drinking Water Science and Technology, Research Centre for Eco-Environmental Sciences, Chinese Academy of Sciences, 100085 Beijing, P. R. China; Section of Sanitary Engineering, Department of Water Management, Faculty of Civil Engineering and Geosciences,*

https://doi.org/10.1021/acs.est.1c07377
Environ. Sci. Technol. 2022, 56, 4988−4997

Delft University of Technology, 2628 CN Delft, The Netherlands

Meng Jiao − *Key Laboratory of Drinking Water Science and Technology, Research Centre for Eco-Environmental Sciences, Chinese Academy of Sciences, 100085 Beijing, P. R. China; University of Chinese Academy of Sciences, 100049 Beijing, P. R. China*

Jan Peter van der Hoek − *Section of Sanitary Engineering, Department of Water Management, Faculty of Civil Engineering and Geosciences, Delft University of Technology, 2628 CN Delft, The Netherlands; Waternet, Department Research & Innovation, 1090 GJ Amsterdam, The Netherlands;* orcid.org/0000-0002-0674-388X

Complete contact information is available at: https://pubs.acs.org/10.1021/acs.est.1c07377

Notes

The authors declare no competing financial interest.

■ ACKNOWLEDGMENTS

The present work was financially supported by the National Key R&D Program of China (2018YFE0204100).

■ REFERENCES

(1) Alimi, O. S.; Farner Budarz, J.; Hernandez, L. M.; Tufenkji, N. Microplastics and Nanoplastics in Aquatic Environments: Aggregation, Deposition, and Enhanced Contaminant Transport. *Environ. Sci. Technol* **2018**, *52*, 1704−1724.

(2) Baptista Neto, J. A.; Gaylarde, C.; Beech, I.; Bastos, A. C.; da Silva Quaresma, V.; de Carvalho, D. G. Microplastics and attached microorganisms in sediments of the Vitória bay estuarine system in SE Brazil. *Ocean Coastal Manag.* **2019**, *169*, 247−253.

(3) Rogers, K. L.; Carreres-Calabuig, J. A.; Gorokhova, E.; Posth, N. R. Micro-by-micro interactions: How microorganisms influence the fate of marine microplastics. *Limnol. Oceanogr. Lett.* **2020**, *5*, 18−36.

(4) Seeley, M. E.; Song, B.; Passie, R.; Hale, R. C. Microplastics affect sedimentary microbial communities and nitrogen cycling. *Nat. Commun.* **2020**, *11*, No. 2372.

(5) Van Melkebeke, M.; Janssen, C.; De Meester, S. Characteristics and Sinking Behavior of Typical Microplastics Including the Potential Effect of Biofouling: Implications for Remediation. *Environ. Sci. Technol.* **2020**, *54*, 8668−8680.

(6) Waldschläger, K.; Schuttrumpf, H. Infiltration Behavior of Microplastic Particles with Different Densities, Sizes, and Shapes-From Glass Spheres to Natural Sediments. *Environ. Sci. Technol* **2020**, *54*, 9366−9373.

(7) Wright, R. J.; Erni-Cassola, G.; Zadjelovic, V.; Latva, M.; Christie-Oleza, J. A. Marine Plastic Debris: A New Surface for Microbial Colonization. *Environ. Sci. Technol.* **2020**, *54*, 11657−11672.

(8) Yuan, W.; Zhou, Y.; Liu, X.; Wang, J. New Perspective on the Nanoplastics Disrupting the Reproduction of an Endangered Fern in Artificial Freshwater. *Environ. Sci. Technol* **2019**, *53*, 12715−12724.

(9) Xu, Y.; He, Q.; Liu, C.; Huangfu, X. Are Micro- or Nanoplastics Leached from Drinking Water Distribution Systems? *Environ. Sci. Technol* **2019**, *53*, 9339−9340.

(10) Amaral-Zettler, L. A.; Zettler, E. R.; Mincer, T. J. Ecology of the plastisphere. *Nat. Rev. Microbiol* **2020**, *18*, 139−151.

(11) Enfrin, M.; Lee, J.; Gibert, Y.; Basheer, F.; Kong, L.; Dumee, L. F. Release of hazardous nanoplastic contaminants due to microplastics fragmentation under shear stress forces. *J. Hazard Mater.* **2020**, *384*, No. 121393.

(12) Liu, P.; Qian, L.; Wang, H.; Zhan, X.; Lu, K.; Gu, C.; Gao, S. New Insights into the Aging Behavior of Microplastics Accelerated by Advanced Oxidation Processes. *Environ. Sci. Technol.* **2019**, *53*, 3579−3588.

(13) Roager, L.; Sonnenschein, E. C. Bacterial Candidates for Colonization and Degradation of Marine Plastic Debris. *Environ. Sci. Technol.* **2019**, *53*, 11636−11643.

(14) Rowenczyk, L.; Dazzi, A.; Deniset-Besseau, A.; Beltran, V.; Goudouneche, D.; Wong-Wah-Chung, P.; Boyron, O.; George, M.; Fabre, P.; Roux, C.; Mingotaud, A. F.; Halle, A. T. Microstructure Characterization of Oceanic Polyethylene Debris. *Environ. Sci. Technol.* **2020**, *54*, 4102−4109.

(15) Gigault, J.; El Hadri, H.; Nguyen, B.; Grassl, B.; Rowenczyk, L.; Tufenkji, N.; Feng, S.; Wiesner, M. Nanoplastics are neither microplastics nor engineered nanoparticles. *Nat. Nanotechnol* **2021**, *16*, 501−507.

(16) Mitrano, D. M.; Wick, P.; Nowack, B. Placing nanoplastics in the context of global plastic pollution. *Nat. Nanotechnol.* **2021**, *16*, 491−500.

(17) Tan, Y.; Zhu, X.; Wu, D.; Song, E.; Song, Y. Compromised Autophagic Effect of Polystyrene Nanoplastics Mediated by Protein Corona Was Recovered after Lysosomal Degradation of Corona. *Environ. Sci. Technol.* **2020**, *54*, 11485−11493.

(18) Thiagarajan, V.; Iswarya, V.; P, A. J.; Seenivasan, R.; Chandrasekaran, N.; Mukherjee, A. Influence of differently functionalized polystyrene microplastics on the toxic effects of P25 TiO2 NPs towards marine algae Chlorella sp. *Aquat. Toxicol.* **2019**, *207*, 208−216.

(19) Brun, N. R.; van Hage, P.; Hunting, E. R.; Haramis, A. G.; Vink, S. C.; Vijver, M. G.; Schaaf, M. J. M.; Tudorache, C. Polystyrene nanoplastics disrupt glucose metabolism and cortisol levels with a possible link to behavioural changes in larval zebrafish. *Commun. Biol.* **2019**, *2*, No. 382.

(20) Gu, W.; Liu, S.; Chen, L.; Liu, Y.; Gu, C.; Ren, H. Q.; Wu, B. Single-Cell RNA Sequencing Reveals Size-Dependent Effects of Polystyrene Microplastics on Immune and Secretory Cell Populations from Zebrafish Intestines. *Environ. Sci. Technol* **2020**, *54*, 3417−3427.

(21) Jacob, H.; Besson, M.; Swarzenski, P. W.; Lecchini, D.; Metian, M. Effects of Virgin Micro- and Nanoplastics on Fish: Trends, Meta-Analysis, and Perspectives. *Environ. Sci. Technol* **2020**, *54*, 4733−4745.

(22) Dong, Z.; Hou, Y.; Han, W.; Liu, M.; Wang, J.; Qiu, Y. Protein corona-mediated transport of nanoplastics in seawater-saturated porous media. *Water Res.* **2020**, *182*, No. 115978.

(23) Liu, Y.; Hu, Y.; Yang, C.; Chen, C.; Huang, W.; Dang, Z. Aggregation kinetics of UV irradiated nanoplastics in aquatic environments. *Water Res.* **2019**, *163*, No. 114870.

(24) Nguyen, T. H.; Tang, F. H. M.; Maggi, F. Sinking of microbial-associated microplastics in natural waters. *PLoS One* **2020**, *15*, No. e0228209.

(25) Oriekhova, O.; Stoll, S. Heteroaggregation of nanoplastic particles in the presence of inorganic colloids and natural organic matter. *Environ. Sci.: Nano* **2018**, *5*, 792−799.

(26) Rummel, C. D.; Jahnke, A.; Gorokhova, E.; Kühnel, D.; Schmitt-Jansen, M. Impacts of Biofilm Formation on the Fate and Potential Effects of Microplastic in the Aquatic Environment. *Environ. Sci. Technol. Lett.* **2017**, *4*, 258−267.

(27) Saavedra, J.; Stoll, S.; Slaveykova, V. I. Influence of nanoplastic surface charge on eco-corona formation, aggregation and toxicity to freshwater zooplankton. *Environ. Pollut.* **2019**, *252*, 715−722.

(28) Shams, M.; Alam, I.; Chowdhury, I. Aggregation and stability of nanoscale plastics in aquatic environment. *Water Res.* **2020**, *171*, No. 115401.

(29) Xu, Y.; Ou, Q.; He, Q.; Wu, Z.; Ma, J.; Huangfu, X. Influence of dissolved black carbon on the aggregation and deposition of polystyrene nanoplastics: Comparison with dissolved humic acid. *Water Res.* **2021**, *196*, No. 117054.

(30) Besseling, E.; Foekema, E. M.; Van Franeker, J. A.; Leopold, M. F.; Kuhn, S.; Bravo Rebolledo, E. L.; Hesse, E.; Mielke, L.; J, I. J.; Kamminga, P.; Koelmans, A. A. Microplastic in a macro filter feeder: Humpback whale Megaptera novaeangliae. *Mar. Pollut. Bull.* **2015**, *95*, 248−252.

(31) Alomar, C.; Deudero, S. Evidence of microplastic ingestion in the shark Galeus melastomus Rafinesque, 1810 in the continental

shelf off the western Mediterranean Sea. *Environ. Pollut.* **2017**, *223*, 223−229.
(32) Mao, Y.; Ai, H.; Chen, Y.; Zhang, Z.; Zeng, P.; Kang, L.; Li, W.; Gu, W.; He, Q.; Li, H. Phytoplankton response to polystyrene microplastics: Perspective from an entire growth period. *Chemosphere* **2018**, *208*, 59−68.
(33) Feng, L. J.; Sun, X. D.; Zhu, F. P.; Feng, Y.; Duan, J. L.; Xiao, F.; Li, X. Y.; Shi, Y.; Wang, Q.; Sun, J. W.; Liu, X. Y.; Liu, J. Q.; Zhou, L. L.; Wang, S. G.; Ding, Z.; Tian, H.; Galloway, T. S.; Yuan, X. Z. Nanoplastics Promote Microcystin Synthesis and Release from Cyanobacterial Microcystis aeruginosa. *Environ. Sci. Technol.* **2020**, *54*, 3386−3394.
(34) Mao, Y.; Li, H.; Gu, W.; Yang, G.; Liu, Y.; He, Q. Distribution and characteristics of microplastics in the Yulin River, China: Role of environmental and spatial factors. *Environ. Pollut.* **2020**, *265*, No. 115033.
(35) Schymanski, D.; Goldbeck, C.; Humpf, H. U.; Furst, P. Analysis of microplastics in water by micro-Raman spectroscopy: Release of plastic particles from different packaging into mineral water. *Water Res.* **2018**, *129*, 154−162.
(36) Johnson, A. C.; Ball, H.; Cross, R.; Horton, A. A.; Jurgens, M. D.; Read, D. S.; Vollertsen, J.; Svendsen, C. Identification and Quantification of Microplastics in Potable Water and Their Sources within Water Treatment Works in England and Wales. *Environ. Sci. Technol.* **2020**, *54*, 12326−12334.
(37) Rios Mendoza, L. M.; Balcer, M. Microplastics in freshwater environments: A review of quantification assessment. *TrAC, Trends Anal. Chem.* **2019**, *113*, 402−408.
(38) Löder, M. G. J.; Kuczera, M.; Mintenig, S.; Lorenz, C.; Gerdts, G. Focal plane array detector-based micro-Fourier-transform infrared imaging for the analysis of microplastics in environmental samples. *Environ. Chem.* **2015**, *12*, 563−581.
(39) Käppler, A.; Windrich, F.; Loder, M. G.; Malanin, M.; Fischer, D.; Labrenz, M.; Eichhorn, K. J.; Voit, B. Identification of microplastics by FTIR and Raman microscopy: a novel silicon filter substrate opens the important spectral range below 1300 cm(-1) for FTIR transmission measurements. *Anal. Bioanal. Chem.* **2015**, *407*, 6791−6801.
(40) Schwaferts, C.; Sogne, V.; Welz, R.; Meier, F.; Klein, T.; Niessner, R.; Elsner, M.; Ivleva, N. P. Nanoplastic Analysis by Online Coupling of Raman Microscopy and Field-Flow Fractionation Enabled by Optical Tweezers. *Anal. Chem* **2020**, *92*, 5813−5820.
(41) Gomiero, A.; Øysæd, K. B.; Palmas, L.; Skogerbø, G. Application of GCMS-pyrolysis to estimate the levels of microplastics in a drinking water supply system. *J. Hazard. Mater.* **2021**, *416*, No. 125708.
(42) Picó, Y.; Barceló, D. Pyrolysis gas chromatography-mass spectrometry in environmental analysis: Focus on organic matter and microplastics. *TrAC, Trends Anal. Chem.* **2020**, *130*, No. 115964.
(43) Fischer, M.; Scholz-Bottcher, B. M. Simultaneous Trace Identification and Quantification of Common Types of Microplastics in Environmental Samples by Pyrolysis-Gas Chromatography-Mass Spectrometry. *Environ. Sci. Technol.* **2017**, *51*, 5052−5060.
(44) Ribeiro, F.; Okoffo, E. D.; O'Brien, J. W.; Fraissinet-Tachet, S.; O'Brien, S.; Gallen, M.; Samanipour, S.; Kaserzon, S.; Mueller, J. F.; Galloway, T.; Thomas, K. V. Quantitative Analysis of Selected Plastics in High-Commercial-Value Australian Seafood by Pyrolysis Gas Chromatography Mass Spectrometry. *Environ. Sci. Technol* **2020**, *54*, 9408−9417.
(45) Zhang, X.; Zhang, H.; Yu, K.; Li, N.; Liu, Y.; Liu, X.; Zhang, H.; Yang, B.; Wu, W.; Gao, J.; Jiang, J. Rapid Monitoring Approach for Microplastics Using Portable Pyrolysis-Mass Spectrometry. *Anal. Chem.* **2020**, *92*, 4656−4662.
(46) Ter Halle, A.; Jeanneau, L.; Martignac, M.; Jarde, E.; Pedrono, B.; Brach, L.; Gigault, J. Nanoplastic in the North Atlantic Subtropical Gyre. *Environ. Sci. Technol.* **2017**, *51*, 13689−13697.
(47) Blancho, F.; Davranche, M.; Hadri, H. E.; Grassl, B.; Gigault, J. Nanoplastics Identification in Complex Environmental Matrices: Strategies for Polystyrene and Polypropylene. *Environ. Sci. Technol.* **2021**, *55*, 8753−8759.
(48) Zhou, X. X.; Hao, L. T.; Wang, H. Y.; Li, Y. J.; Liu, J. F. Cloud-Point Extraction Combined with Thermal Degradation for Nanoplastic Analysis Using Pyrolysis Gas Chromatography-Mass Spectrometry. *Anal. Chem.* **2019**, *91*, 1785−1790.
(49) Zhou, X. X.; He, S.; Gao, Y.; Chi, H. Y.; Wang, D. J.; Li, Z. C.; Yan, B. Quantitative Analysis of Polystyrene and Poly(methyl methacrylate) Nanoplastics in Tissues of Aquatic Animals. *Environ. Sci. Technol.* **2021**, *55*, 3032−3040.
(50) Mintenig, S. M.; Bäuerlein, P. S.; Koelmans, A. A.; Dekker, S. C.; van Wezel, A. P. Closing the gap between small and smaller: towards a framework to analyse nano- and microplastics in aqueous environmental samples. *Environ. Sci.: Nano* **2018**, *5*, 1640−1649.
(51) Hurley, R. R.; Lusher, A. L.; Olsen, M.; Nizzetto, L. Validation of a Method for Extracting Microplastics from Complex, Organic-Rich, Environmental Matrices. *Environ. Sci. Technol.* **2018**, *52*, 7409−7417.
(52) Li, X.; Chen, L.; Ji, Y.; Li, M.; Dong, B.; Qian, G.; Zhou, J.; Dai, X. Effects of chemical pretreatments on microplastic extraction in sewage sludge and their physicochemical characteristics. *Water Res.* **2020**, *171*, No. 115379.
(53) Yan, Z.; Zhao, H.; Zhao, Y.; Zhu, Q.; Qiao, R.; Ren, H.; Zhang, Y. An efficient method for extracting microplastics from feces of different species. *J. Hazard Mater.* **2020**, *384*, No. 121489.
(54) Nuelle, M. T.; Dekiff, J. H.; Remy, D.; Fries, E. A new analytical approach for monitoring microplastics in marine sediments. *Environ. Pollut.* **2014**, *184*, 161−169.
(55) Okoffo, E. D.; Ribeiro, F.; O'Brien, J. W.; O'Brien, S.; Tscharke, B. J.; Gallen, M.; Samanipour, S.; Mueller, J. F.; Thomas, K. V. Identification and quantification of selected plastics in biosolids by pressurized liquid extraction combined with double-shot pyrolysis gas chromatography-mass spectrometry. *Sci. Total. Environ.* **2020**, *715*, No. 136924.
(56) Dümichen, E.; Eisentraut, P.; Bannick, C. G.; Barthel, A. K.; Senz, R.; Braun, U. Fast identification of microplastics in complex environmental samples by a thermal degradation method. *Chemosphere* **2017**, *174*, 572−584.
(57) Cowger, W.; Booth, A. M.; Hamilton, B. M.; Thaysen, C.; Primpke, S.; Munno, K.; Lusher, A. L.; Dehaut, A.; Vaz, V. P.; Liboiron, M.; Devriese, L. I.; Hermabessiere, L.; Rochman, C.; Athey, S. N.; Lynch, J. M.; De Frond, H.; Gray, A.; Jones, O. A. H.; Brander, S.; Steele, C.; Moore, S.; Sanchez, A.; Nel, H. Reporting Guidelines to Increase the Reproducibility and Comparability of Research on Microplastics. *Appl. Spectrosc.* **2020**, *74*, 1066−1077.
(58) Shruti, V. C.; Perez-Guevara, F.; Kutralam-Muniasamy, G. Metro station free drinking water fountain- A potential "microplastics hotspot" for human consumption. *Environ. Pollut.* **2020**, *261*, No. 114227.
(59) Lai, Y.; Dong, L.; Li, Q.; Li, P.; Hao, Z.; Yu, S.; Liu, J. Counting Nanoplastics in Environmental Waters by Single Particle Inductively Coupled Plasma Mass Spectroscopy after Cloud-Point Extraction and In Situ Labeling of Gold Nanoparticles. *Environ. Sci. Technol.* **2021**, *55*, 4783−4791.
(60) Materić, D.; Kasper-Giebl, A.; Kau, D.; Anten, M.; Greilinger, M.; Ludewig, E.; van Sebille, E.; Rockmann, T.; Holzinger, R. Micro- and Nanoplastics in Alpine Snow: A New Method for Chemical Identification and (Semi)Quantification in the Nanogram Range. *Environ. Sci. Technol.* **2020**, *54*, 2353−2359.
(61) Gangadoo, S.; Owen, S.; Rajapaksha, P.; Plaisted, K.; Cheeseman, S.; Haddara, H.; Truong, V. K.; Ngo, S. T.; Vu, V. V.; Cozzolino, D.; Elbourne, A.; Crawford, R.; Latham, K.; Chapman, J. Nano-plastics and their analytical characterisation and fate in the marine environment: From source to sea. *Sci. Total Environ.* **2020**, *732*, No. 138792.
(62) Li, C.; Busquets, R.; Campos, L. C. Assessment of microplastics in freshwater systems: A review. *Sci. Total Environ.* **2020**, *707*, No. 135578.

https://doi.org/10.1021/acs.est.1c07377
Environ. Sci. Technol. 2022, 56, 4988−4997

(63) Li, J.; Liu, H.; Paul Chen, J. Microplastics in freshwater systems: A review on occurrence, environmental effects, and methods for microplastics detection. *Water Res.* **2018**, *137*, 362−374.
(64) Koelmans, A. A.; Mohamed Nor, N. H.; Hermsen, E.; Kooi, M.; Mintenig, S. M.; De France, J. Microplastics in freshwaters and drinking water: Critical review and assessment of data quality. *Water Res.* **2019**, *155*, 410−422.
(65) Goeppert, N.; Goldscheider, N. Experimental field evidence for transport of microplastic tracers over large distances in an alluvial aquifer. *J. Hazard. Mater.* **2021**, *408*, No. 124844.
(66) Johnson, W. P.; Rasmuson, A.; Ron, C.; Erickson, B.; VanNess, K.; Bolster, D.; Peters, B. Anionic nanoparticle and microplastic non-exponential distributions from source scale with grain size in environmental granular media. *Water Res.* **2020**, *182*, No. 116012.
(67) Zhang, L.; Liu, J.; Xie, Y.; Zhong, S.; Yang, B.; Lu, D.; Zhong, Q. Distribution of microplastics in surface water and sediments of Qin river in Beibu Gulf, China. *Sci. Total Environ.* **2020**, *708*, No. 135176.
(68) Kaiser, D.; Kowalski, N.; Waniek, J. J. Effects of biofouling on the sinking behavior of microplastics. *Environ. Res. Lett.* **2017**, *12*, No. 124003.
(69) Leiser, R.; Wu, G. M.; Neu, T. R.; Wendt-Potthoff, K. Biofouling, metal sorption and aggregation are related to sinking of microplastics in a stratified reservoir. *Water Res* **2020**, *176*, No. 115748.
(70) Michels, J.; Stippkugel, A.; Lenz, M.; Wirtz, K.; Engel, A. Rapid aggregation of biofilm-covered microplastics with marine biogenic particles. *Proc. R. Soc. B* **2018**, *285*, No. 20181203.
(71) Gorski, G.; Fisher, A. T.; Beganskas, S.; Weir, W. B.; Redford, K.; Schmidt, C.; Saltikov, C. Field and Laboratory Studies Linking Hydrologic, Geochemical, and Microbiological Processes and Enhanced Denitrification during Infiltration for Managed Recharge. *Environ. Sci. Technol.* **2019**, *53*, 9491−9501.
(72) Hidalgo-Ruz, V.; Gutow, L.; Thompson, R. C.; Thiel, M. Microplastics in the marine environment: a review of the methods used for identification and quantification. *Environ. Sci. Technol.* **2012**, *46*, 3060−3075.
(73) Du, J.; Xu, S.; Zhou, Q.; Li, H.; Fu, L.; Tang, J.; Wang, Y.; Peng, X.; Xu, Y.; Du, X. A review of microplastics in the aquatic environmental: distribution, transport, ecotoxicology, and toxicological mechanisms. *Environ. Sci. Pollut. Res. Int.* **2020**, *27*, 11494−11505.
(74) Eerkes-Medrano, D.; Thompson, R. C.; Aldridge, D. C. Microplastics in freshwater systems: a review of the emerging threats, identification of knowledge gaps and prioritisation of research needs. *Water Res.* **2015**, *75*, 63−82.
(75) Qian, J.; Tang, S.; Wang, P.; Lu, B.; Li, K.; Jin, W.; He, X. From source to sink: Review and prospects of microplastics in wetland ecosystems. *Sci. Total Environ.* **2021**, *758*, No. 143633.
(76) Pivokonsky, M.; Cermakova, L.; Novotna, K.; Peer, P.; Cajthaml, T.; Janda, V. Occurrence of microplastics in raw and treated drinking water. *Sci. Total Environ.* **2018**, *643*, 1644−1651.
(77) Hernandez, L. M.; Xu, E. G.; Larsson, H. C. E.; Tahara, R.; Maisuria, V. B.; Tufenkji, N. Plastic Teabags Release Billions of Microparticles and Nanoparticles into Tea. *Environ. Sci. Technol.* **2019**, *53*, 12300−12310.
(78) Alimi, O. S.; Farner, J. M.; Tufenkji, N. Exposure of nanoplastics to freeze-thaw leads to aggregation and reduced transport in model groundwater environments. *Water Res.* **2021**, *189*, No. 116533.
(79) Li, Y.; Wang, X.; Fu, W.; Xia, X.; Liu, C.; Min, J.; Zhang, W.; Crittenden, J. C. Interactions between nano/micro plastics and suspended sediment in water: Implications on aggregation and settling. *Water Res.* **2019**, *161*, 486−495.
(80) Liu, Y.; Huang, Z.; Zhou, J.; Tang, J.; Yang, C.; Chen, C.; Huang, W.; Dang, Z. Influence of environmental and biological macromolecules on aggregation kinetics of nanoplastics in aquatic systems. *Water Res.* **2020**, *186*, No. 116316.
(81) Wang, X.; Zheng, H.; Zhao, J.; Luo, X.; Wang, Z.; Xing, B. Photodegradation Elevated the Toxicity of Polystyrene Microplastics to Grouper (Epinephelus moara) through Disrupting Hepatic Lipid Homeostasis. *Environ. Sci. Technol.* **2020**, *54*, 6202−6212.

NOTE ADDED AFTER ASAP PUBLICATION

This paper was published on April 4, 2022. Due to production error, an incorrect graphic was used as Figure 4. The corrected version was reposted on April 4, 2022.

https://doi.org/10.1021/acs.est.1c07377
Environ. Sci. Technol. 2022, 56, 4988−4997